ACS OMEGA

Open Access

http://pubs.acs.org/journal/acsodf

Article

Wide Bandwidth High-Power Triboelectric Energy Harvesting by Scotch Tape

Moon-Hyung Jang,* Sean P. Rabbitte, Abdelkader Frendi, Ryan T. Conners, Yu Lei, and Gang Wang*

Cite This: ACS Omega 2025, 10, 2778−2789

Read Online

ACCESS | Metrics & More | Article Recommendations | Supporting Information

ABSTRACT: A triboelectric generator was proposed using commercial tape materials, which are composed of metalized poly(ethylene terephthalate) films to serve as electrodes and Scotch tape layers for power generation. Power extraction is achieved by the interaction between polypropylene and the acrylic adhesive layer when pressing and releasing, in which the atomic size gaps are formed due to van der Waals forces at the interface. The proposed triboelectric generator was sandwiched between two plastic plates to lead to a vibration-based energy harvester design with a mass attached to the top. Shaker tests were conducted by varying the vibration frequency, tape layer, and type. A peak power of 45 mW was reached at 40 Hz when using two long-lasting tape layers. The acrylic adhesive layer of long-lasting tape is thicker than other Scotch tapes, which results in higher power generation by the narrowing of atomic gaps. Combining two long-lasting tape layers and two box-lock tape layers produced a 53 mW peak power. Powering of a laser diode was demonstrated at 120 Hz. Current triboelectric generator concept can be applied to a biosensor and acoustic sensor design, as demonstrated in the paper as well.

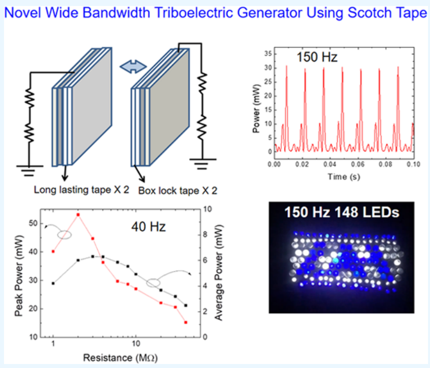

■ INTRODUCTION

Off-grid small-scale energy-harvesting devices can utilize environmental, mechanical energy to operate low-power-profile electronic systems in various applications. These include structural health monitoring, wearable sensors, and other monitoring systems. Ideally, these should be stand-alone systems with the capability to harvest ambient mechanical energy and convert it into electricity to power themselves unimpeded. Also, these systems should have a low environmental impact.[1−7] Triboelectricity has been introduced as an energy-harvesting device that generates power by electrostatic charges through the friction of two surfaces with different materials. Since its invention in 2012, the triboelectric nanogenerator (TENG) is one of the most promising candidates for small-scale energy harvesters.[6,7] This process converts mechanical energy into electrical energy using the triboelectric effect and electrostatic charges. In this method, the electrical potential is generated by the charge transfer between two thin triboelectric layers with opposite polarities when a contact is made. Triboelectric layers can be chosen from various combinations of materials from the triboelectric series to maximize power generation. For example, Cu and Poly(tetrafluoroethylene) (PTFE: Teflon) combination/Poly(methyl methacrylate) (PMMA) and polyimide (Kapton) combination can be chosen for positive and negative triboelectric layers.[8,9] Those combinations can generate electrical currents by touching each other such as contact separation and sliding. Along with a proper external circuit, electrons can flow between two electrodes on the back side of the layers to equalize the electrical potential.

Currently, researchers have focused on applying new materials, including metal−organic frameworks (MOFs), hydrogels, liquids, and even plastic waste. Pandey et al.[10] synthesized zeolite imidazolate framework 8 (ZIF-8) MOFs on polyacrylonitrile (PAN) nanofiber surfaces with a positive triboelectric layer with a poly(tetrafluoroethylene) (PTFE) negative layer for high-performance TENGs. Despite being based on a new material platform, the power density value is low, at 1.91 W/m^2. Rahman et al.[11] synthesized MOF-derived cobalt-based nanoporous carbon (Co-NPC) for incorporation into poly(vinylidene fluoride) (PVDF) composite nanofibers. These nanofiber mats were the negative triboelectric layer, whereas nylon-11 nanofiber mats were used as the positive triboelectric layer for contact and separation configurations. It showed a high-power density of 19.24 W/m^2. However, the applied frequency is only up to 12 Hz, which may not be sufficient for various sensing applications. Applying ZIF-8 into hydrogel was reported to develop stretchable electrodes for wearable TENGs.[12] ZIF-8 was incorporated as a reinforcing nanofiller into poly(acrylamide)-co-hydroxyethyl acrylate (PAAm-*co*-HEA) hydrogel with LiCl electrolyte. The nitrile glove and silicone layers were the positive and negative

Received: September 18, 2024
Revised: December 19, 2024
Accepted: December 25, 2024
Published: January 13, 2025

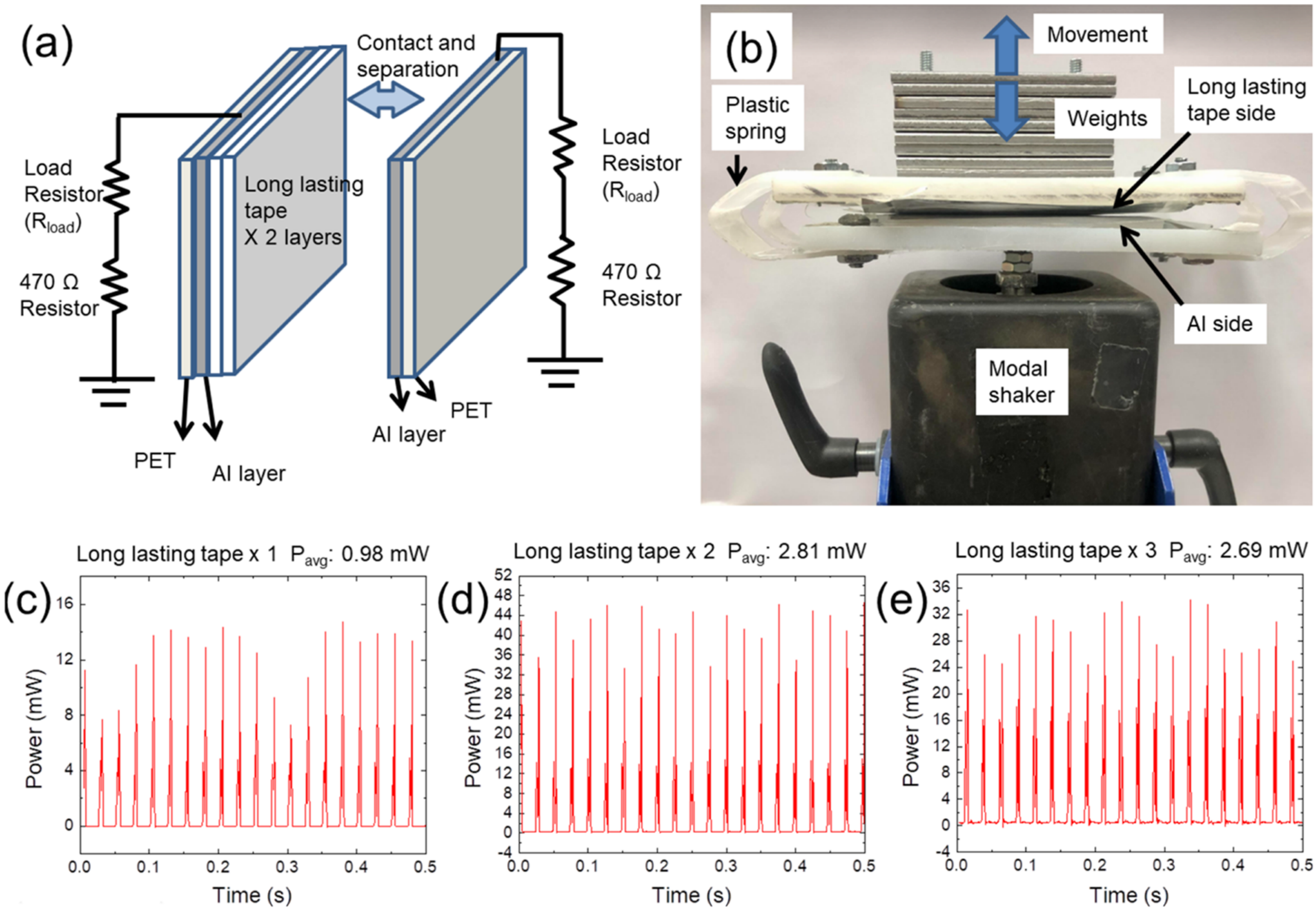

Figure 1. (a) Schematic of configuration for PET/Al/long-lasting tape/long-lasting tape − Al/PET. (b) Actual VBEH device for a vertical motion by modal shaker and weights on the top. Power generation by (c) one tape layer − Al/PET, (d) two layers of tape − Al/PET, and (e) three layers of tape − Al/PET at 40 Hz.

triboelectric layers, respectively. Power density and frequency are up to 3.47 W/m^2 and 4 Hz. Navaneeth et al.[13] utilized medical plastic waste such as saline bottle sheets (polyethylene) along with silicone sheets for the positive and negative triboelectric layers in contacting and separating configurations, respectively. It showed a significant power output at 8.78 W/m^2. However, the frequency was limited to 5 Hz. Therefore, efforts to apply new material systems provide good insight into the evolution of triboelectric systems while also realizing that there are many facts to consider for the successful adoption of new materials.

Our previous results show a novel triboelectric generator based on a simple configuration involving double-sided tape or limestone putty with a poly(ethylene terephthalate) (PET) coated with Aluminum (Al) film.[14,15] Power generation was achieved by contact separation between the double-sided tape or limestone mounting paste and the PET/Al layer. Air breakdown via an electric spark between triboelectric layers removes the charges in the triboelectric layers so that electrons from the ground flow to the Al layer. Al/PET/double-sided tape-PET/Al shows performance comparable to that of the TENGs in the literature. For example, 476 LEDs were turned on using a 38 mm × 25 mm size generator. The operating frequency range of those triboelectric generators was up to 60 Hz. Direct powering of a 650 nm laser diode was also demonstrated. However, because the bond between the triboelectric layers was very strong, the operation required strong pushing and pulling forces. Therefore, it is necessary to produce a similar amount of electrical energy with a smaller force. Moreover, the frequency bandwidth is limited due to the tackiness of the triboelectric layer in such a design.

In this paper, an innovative triboelectric generator was proposed using Commercial off-the-shelf (COTS) Scotch tapes for energy harvesting via the triboelectric effect, which is composed of PET/Al films and multiple Scotch brand tape layers. The PET/Al film serves as electrode layers, and the power generation is achieved by exploring the interaction between the tape polypropylene (PP) backing material and the acrylic adhesive layer when pressing and releasing, as reported in our previous work,[14] in which a single Scotch tape layer was used. The polypropylene surface only has partial positive charges because of a nonpolar surface, while the acrylic adhesive has a polar surface with positively and negatively charged and neutral regions. Atomic size gaps are formed because of the attractive and repulsive areas at the interface due to van der Waals forces. In current work, the contact surface was not sticky as previously reported for double-sided tape generators.[14] The smooth surface allows the generator to operate at a much higher frequency, which leads to a wide bandwidth and high-performance triboelectric energy-harvesting concept. In addition, our design is low cost and easy to build without using the nanotechnology schemes for typical TENG fabrication.

https://doi.org/10.1021/acsomega.4c08590
ACS Omega 2025, 10, 2778−2789

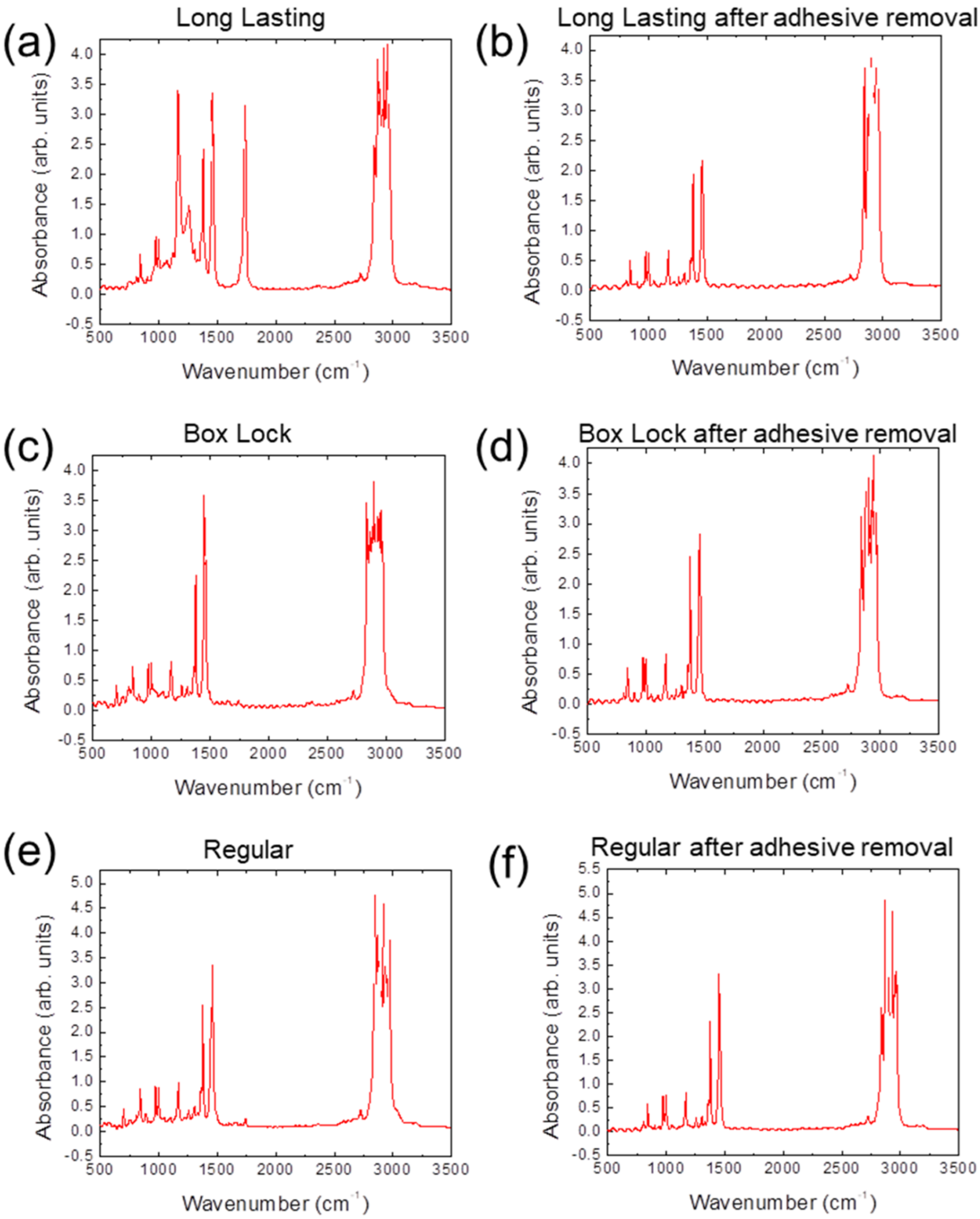

Figure 2. FTIR spectra of Scotch long- lasting tape (a) before and (b) after removing the adhesive layer, Scotch box-lock tape (c) before and (d) after removing the adhesive layer, and Scotch regular shipping tape (e) before and (f) after removing adhesive layer.

The first triboelectric generator configuration was assembled as PET/Al/Scotch long-lasting tape/Scotch long-lasting tape-PET/Al. Such an assembly is integrated into a vibration-based energy harvester (VBEH) design, which was sandwiched between two three-dimensional (3D)-printed plastic plates connected by plastic springs. Note that the VBEH design was adopted in our demonstration because the configuration is simple and easy to build. A proof mass was attached to the top plate, and the bottom plate was interfaced with a vibration source. We conducted comprehensive shaker tests to evaluate the VBEH performance by varying the vibration frequency, Scotch tape layer number and type (i.e., long lasting or box lock), and electric loads. A peak power of 45 mW over an area of 50 mm × 70 mm was obtained at 40 Hz, which corresponds to a power density of 12.86 W/m^2. Because the acrylic adhesive layer of long-lasting tape is much thicker than other Scotch tapes, the atomic gap between the acrylic adhesive and the PP backing layer was much narrower than that of other Scotch tapes. Narrowing the atomic gap creates more localized contact and separation between the acrylic adhesive and PP, producing a high output. The peak power was further increased by introducing Scotch brand box-lock tape in our triboelectric generator design. The optimized configuration in a VBEH system is PET/Al/long-lasting tape/long-lasting tape -

https://doi.org/10.1021/acsomega.4c08590
ACS Omega 2025, 10, 2778−2789

box-lock tape/box-lock tape/Al/PET, producing 53 mW peak power at 40 Hz and delivering a power density of 15.14 W/m^2.

The bandwidth of the VBEH was significantly increased because we leveraged the inherent triboelectric effect between the PP backing layer and the acrylic adhesive layer in a tape instead of involving the interface with the tacky layer in our previous work.[14,15] It was shown that the peak power values of 30 and 2.5 mW were achieved at 150 and 300 Hz, respectively. Direct powering of 148 LEDs and a 650 nm laser diode was demonstrated using our VBEH at 150 and 120 Hz, respectively.

Additionally, we extended our triboelectric generator to sensor applications by adopting an optimized triboelectric configuration. A self-powered wearable biosensor was developed to conduct human motion tracking. The newly proposed triboelectric configuration eliminates the direct tape interface with human skin, which could result in skin irritation and sensor degradation due to sweat. The no-skin contact design allows us to obtain clean and consistent signals to reflect the human body motion. Moreover, a triboelectric acoustic sensor prototype was developed. Sound can be recorded and recorded between the speaker and the sensor system over various distances.

In summary, the Scotch tape-based triboelectric generator concept was proposed and integrated into a VBEH design for an energy-harvesting demonstration with wide bandwidth performance. In addition, such triboelectric generators can be applied to acoustic and human body sensing applications, as demonstrated in our acoustic sensor and biosensor prototype, respectively. Detailed description and discussion are included in the following sections.

■ EXPERIMENTAL SETUP

Preparation of Triboelectric Generator and Electrical Characterization. Figure 1 shows the experimental setup for the VBEH shaker test. Figure 1(a) shows the schematic of the proposed triboelectric generator system, in which two layers of long-lasting tape were attached to the Al/PET film on one side. On the other hand, an Al/PET layer was used. Note that Scotch brand box-lock tape/box-lock tape/Al/PET assembly was used for other configurations. The active area was 50 mm × 70 mm. Instead of measuring typical open circuit voltage (V_{OC}) and short circuit current (I_{SC}), we introduced a 470 Ω resistor in the circuit to characterize power from voltage measurements and current data. Both Al layers served as electrodes in a circuit with an electrode load (R_{load}), which was connected in series to this 470 Ω resistor.[14] The voltage data over this 470 Ω resistor was recorded using a multichannel oscilloscope. Then, the current values in this series circuit can be determined based on Ohm's law. Finally, we can obtain the total power in the circuit to evaluate the energy harvester performance. The electrical load (R_{load}) was set to 2 MΩ for the power calculations. A digital oscilloscope (1008A 8-channel USB digital oscilloscope, Hantek) was used to collect voltage signals. Figure 1(b) shows a VBEH prototype, in which the side with two long-lasting tape layers was attached to a 3-D printed acrylic top plate using foam tape, and the side with Al/PEF was attached to the bottom plate. The gap between the two plates was adjusted accordingly to enable contact and separate motion when the bottom plate was under vibration. Four PP plastic springs were used to connect both the top and bottom plates at the four corners. A proof mass was attached to the top of the acrylic plate to provide sufficient compressive force during the contact process and to tune the system resonance frequency if needed. Total VBEH system weights at 610 g. The VBEH prototype was screwed into a modal shaker head (Smart Shaker 2007E01 from The Modal Shop, Inc.). The VBEH was driven in the frequency range of 30−300 Hz. The LED array (148 to 366 pieces) was also connected to the VBEH via a bridge rectifier (Four FR107 diodes) for LED lighting demonstration. Direct powering of a diode laser (wavelength at 650 nm) was also demonstrated at various frequencies from 30 to 120 Hz. Amplitude change in the laser was observed using a DET100A2 photodetector (Thorlabs, Inc.) with a 320−1100 nm spectral range.

Tape Materials Characterization. Fourier transform infrared (FTIR) spectral measurements were performed on Scotch brand long lasting, box lock, and regular shipping tapes before and after removing the acrylic adhesive layer using a Nicolet IR100 FTIR spectrometer (Thermo Fisher Scientific) as shown in Figure 2. Adhesive removal was performed with clean wipes of the isopropanol lens. The purpose was to identify the characteristics of the acrylic adhesive layer in order to design an optimal triboelectric generator. The optimized configuration in a VBEH system was PET/Al/long-lasting tape/long-lasting tape: box-lock tape/box-lock tape/Al/PET.

Sensors Characterization. The optimized triboelectric generator configuration was assumed to be used to develop a wearable biosensor. The entire assembly was placed without a gap between two cloth covers on the forearm for a human body motion tracking demonstration. Two separate electrical wires were connected to each Al layer. An acoustic sensor prototype was developed based on the same optimized triboelectric generator configuration. There was no physical gap between those layers in the assembly, and the active sensing area was 60 mm × 60 mm. The triboelectric assembly was attached to a 3-D printed vertical stand for acoustic sensing. The signal wire was attached to the Al layer on the side with long-lasting tape layers, and the ground wire was attached to the Al layer on the side with box-lock tape layers. A Bluetooth speaker was placed in front of the sensor to serve as an acoustic input, and signals were collected at different distances between the speaker and the sensor system. The signal was passed to a digital oscilloscope for the amplitude measurements. To record sound files, the signal was connected to a DIGITNOW phono turntable preamplifier. The preamplifier's output was routed to a laptop computer via the auxiliary connector for recording sound files.

■ RESULTS AND DISCUSSION

Figure 1(a) shows the schematic of PET/Al/long-lasting tape/long-lasting tape − Al/PET triboelectric layer configuration for contact and separation process. It was assembled into a modal shaker as shown in Figure 1(b) for the VBEH operation. Operation of VBEH with voltage amplitude measurements at various frequencies was recorded, as shown in Supporting (Movie S1). Time history plots of power generation are shown in Figure 1(c)−(e) when the number of long-lasting tape layers varies from one to three. The shaker input frequency was set at 40 Hz. Peak power was 14 mW when there was only one tape layer. Then, by adding one more layer, peak power abruptly increased to 45 mW. When increasing to three layers, peak power decreased to 33 mW. The average power (P_{avg}) of one, two, and three tape layers was 0.98, 2.81, and 2.69 mW, respectively as shown in Figure 1(c)−(e).

https://doi.org/10.1021/acsomega.4c08590
ACS Omega 2025, 10, 2778−2789

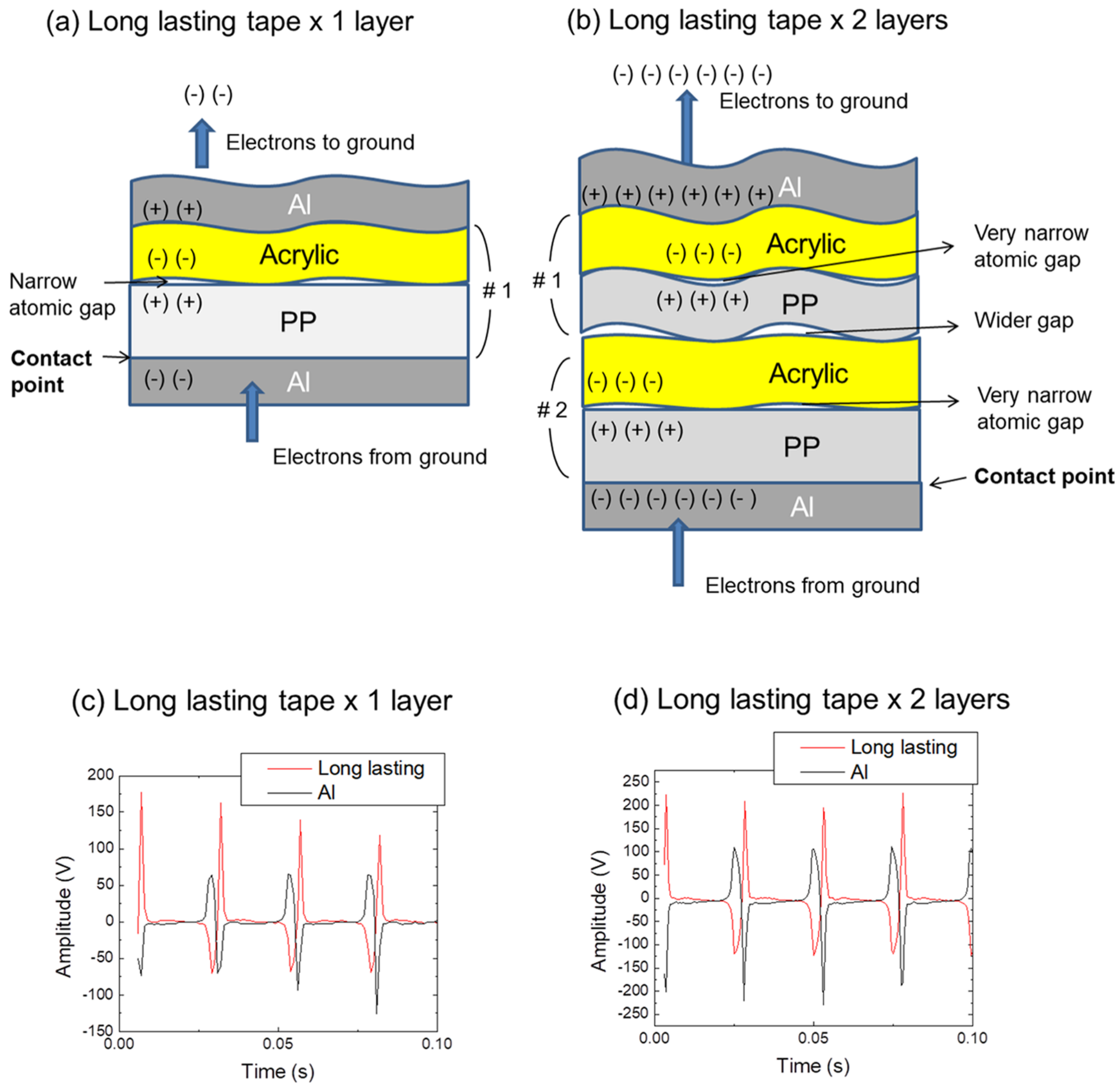

Figure 3. Schematics of (a) Al/long-lasting tape (#1) − Al configuration during the contact process. (b) Al/long-lasting tape (#1) /long-lasting tape (#2) − Al configuration. Voltage amplitude generation from long-lasting tape side (red) and Al side (black) as a function of time for (c) Al/long-lasting tape − Al configuration and (d) Al/long-lasting tape/long-lasting tape − Al configurations.

The number of tape layers, i.e., tape assembly thickness, plays a crucial role in power generation. As mentioned above, the physics behind the current VBEH was to leverage the interaction between the PP backing layer and the acrylic adhesive layer. Therefore, we needed to determine the characteristics of the acrylic adhesive layer since it contributes significantly to power generation. Figure 2 shows the FTIR spectra of three Scotch brand tapes with and without an adhesive layer. Figure 2(a),(b) shows the FTIR spectra of long-lasting tape before and after the removal of the acrylic adhesive, respectively. In long-lasting tape, the spectral properties before and after the removal of the adhesive layer are significantly different. It shows the spectral characteristics of the acrylic adhesive layer before removal, along with the peaks of the PP substrate layer.[16] The acrylic peak in the range 1000−1500 cm^{-1} changes significantly after adhesive removal, while the peak spectra of the PP material remain almost the same. However, in the case of box locks and general shipping tapes, there was no significant change in peaks even after removing the adhesive layer. These results strongly indicate that the acrylic adhesive layer in long-lasting tapes is much thicker than that of the other tapes. Additionally, the peaks of the PP backing layer appear to be almost the same after adhesive removal. Therefore, it is reasonable to conclude that the thick acrylic layer in long-lasting tape is responsible for the high-power generation in a VBEH system. In other words, the use of long-lasting tape is preferred for power generation in the current design.

Our previous study on regular Scotch tape biosensors has shown that an atomic gap is created between the acrylic adhesive and the polypropylene support by forming density-depleted regions because the acrylic layer shows positive, neutral, and negative charges while the PP layer only provides positive charges.[17,18] When tensile or compressive stress is applied to a scotch tape, an electrical signal is generated due to a change in the height of the atomic gap.[17] Likewise, long-lasting tapes create atomic gaps between the acrylic and PP layers, as shown in Figure 3(a). The thickness of the acrylic layer is much bigger than that of regular Scotch tapes, so the height of the atomic gap becomes narrower during the production process. Therefore, the narrow atomic gap can actually help power generation during contact and separation

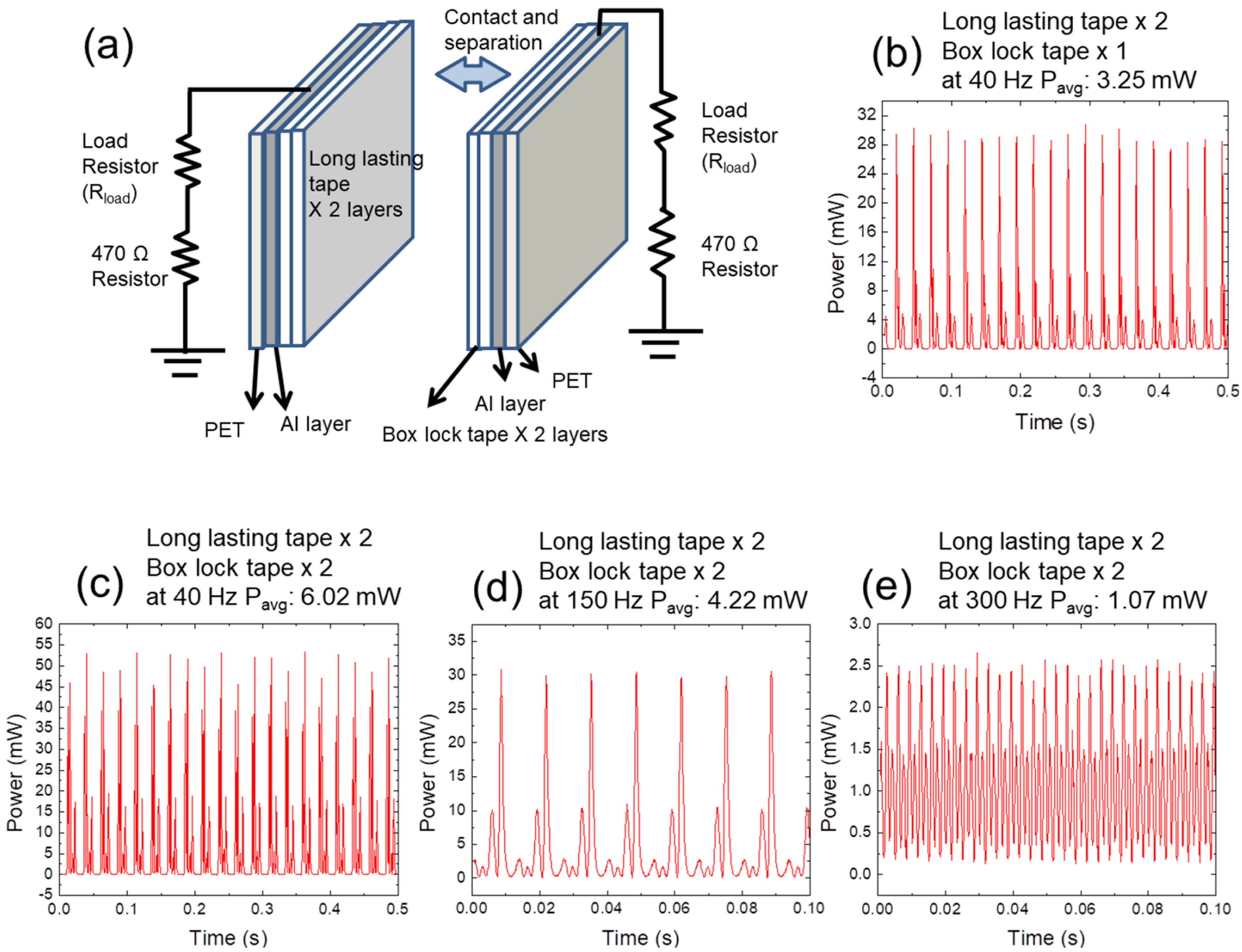

Figure 4. (a) Schematic of a triboelectric generator with two different Scotch tapes as triboelectric layers. The configuration is PET/Al/long-lasting tape/long-lasting tape − box-lock tape/box-lock tape/Al/PET. Power generation results with (b) two long-lasting tape layers and one box-lock tape layer, (c) two long-lasting tape and two box-lock tape layers at 40 Hz and two long-lasting tape and two box-lock tape layers at (d) 150 Hz and (e) 300 Hz.

motion. In the contact process, triboelectric charges are generated as acrylic and PP layers come into contact, as shown in Figure 3(a). The separation process recombines the charges in the gap, as previous research has reported on a Scotch tape emitting X-rays in a vacuum when separating the acrylic and PP layers.[19] This helps the triboelectric generator operate very quickly, up to 300 Hz, as no charge remains after the separation process. More importantly, adding more layers of tape creates more charges, as shown in Figure 3(b).

In reality, these atomic gaps are localized and randomly distributed at the interface between the acrylic and the PP layer.[18] This indicates that the charges generated in the gap do not block the charges on other interfaces. Moreover, the interface between two individual long-lasting tapes creates a wider atomic gap that does not contribute to charge generation. Rather, it pushes the acrylic and PP layers outward, causing the atomic gap to become even narrower. Therefore, adding two layers increases peak power by a factor of 3, as shown in Figure 1(d). However, adding three layers of tape reduces the power because the distance from the electrode is much greater and the VBEH impact is weakened at the atomic gaps. Even without a tacky interface between the two triboelectric layers, the current PET/Al/long-lasting tape/long-lasting tape - Al/PET configurations have a high power at higher frequencies because the built-in narrow gap creates a charge on the interface between the acrylic adhesive layer and PP backing layer. Power time history data are plotted in Figure 3(c,d) when using one and two long-lasting tape layers, respectively. Note that a negative voltage was developed on the long-lasting tape side, which is expected because the electron flow on the tape side is toward the ground.

Further development on higher power generation was conducted. We added Scotch brand box-lock tape layers on the Al/PET side, as shown in Figure 4(a). Therefore, additional power generation was expected since more layers of tape material were introduced. Time history plots of power generation are shown in Figure 4(b,c) when the box-lock tape layer varies from one to two. Interestingly, the peak power values were about 30 and 53 mW, respectively. Wang et al.[20] reported 2.16 mW average power and Chung et al.[21] showed average power of 3.91 mW in contact-and-separate TENG (CS-TENG). Our average power increases from 2.81 mW (Figure 1(d)) to 3.25 and 6.02 mW after adding one and two layers of box-locking tape, respectively. Our average power

https://doi.org/10.1021/acsomega.4c08590
ACS Omega 2025, 10, 2778−2789

results show comparable or higher value compared to the case of CS-TENG studies.[20,21] Current results also indicate that power generation can be improved after introducing different kinds of tape materials on the other side. We tested the triboelectric generator with the configuration of PET/Al/long-lasting tape/long-lasting tape/long-lasting tape/Al/PET, and the power generation was minimal. Since the adhesive layer was much thicker in long-lasting tape, adding two identical layers on the opposite side will decrease the power as the distance to Al (conductor) increases, as in the previous case with three long-lasting tape layers.

In addition, power generation demonstration was conducted at higher frequencies as shown in Figure 4(d),(e) for the cases of 150 and 300 Hz, respectively. At 150 Hz, it still shows decent amount of peak power at 30 mW, while the peak power was reduced significantly to 2.5 mW at 300 Hz. Average power values were reduced from 4.22 to 1.07 mW. Since small-scale energy-harvesting devices, such as wearable exoskeleton systems, require a wider frequency bandwidth for power generation, the capability of generating power at such high frequencies would be beneficial.

Both peak and average power as a function of electrical load (R_{load}) are shown in Figure 5 with the triboelectric configuration of PET/Al/long-lasting tape/long-lasting tape − box-lock tape/box-lock tape/Al/PET. Time history plots of power under different electrical loads are shown in Supporting Figure S1. Peak power reached the maximum value at 2 MΩ and gradually decreased to 15 mW at 40 MΩ. The average power value did not show much variation when increasing the electrical load from 2 to 10 MΩ. This indicated that the current configuration can tolerate a wider electrical load range without much degradation for power generation.

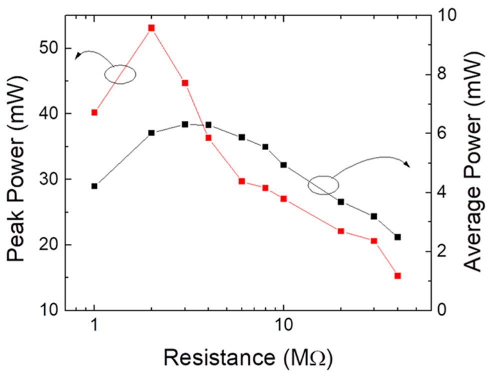

Figure 5. Peak power (red) and average power (black) versus electrical load (impedance) at 40 Hz of the VBEH operation frequency.

Table 1 shows a performance comparison in terms of power density and frequency for recent CS-TENG concepts using novel materials. Note that the power density is calculated by the ratio between peak power and active area. Maximum power density reaches to 32.03 W/m^2 at 2 Hz, in which natural boron minerals (NBO) doped silicone was used.[22] Power density of our triboelectric generator prototypes varies from 0.43 W/m^2 at 300 Hz to 15.14 W/m^2 at 40 Hz. The highest frequency of recent CS-TENG devices is 12 Hz while our triboelectric generator can operate from 40 to 300 Hz. Therefore, our design shows comparable capability of power generation with a significantly higher operational frequency. Moreover, only commercial off-the-shelf tape materials and a simple fabrication scheme are adopted in our design.

Direct powering of LEDs and a laser diode was demonstrated as well, and a bridge rectifier circuit was used to convert AC power to DC.[14] Figure 6 shows the results of powering LEDs under 150, 20, and 40 Hz. Corresponding video clips at 150, 20, and 40 Hz are provided in Supporting

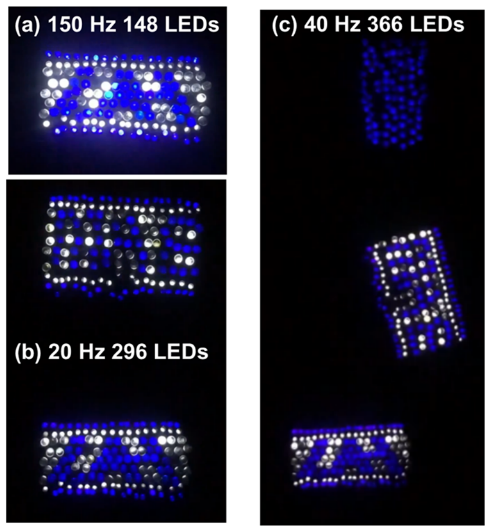

Figure 6. LED lighting at (a) 150 Hz, (b) 20 Hz, and (c) 40 Hz VBEH frequencies with 148, 296, and 366 LEDs, respectively.

Table 1. Recent Progresses in TENG Design with Novel Materials

reports	new materials	power density (W/m^2)	frequency (Hz)
Pandey et al.[10]	zeolite imidazolate framework 8 (ZIF-8) MOFs on polyacrylonitrile (PAN) nanofiber	1.91	12
Rahman et al.[11]	MOF-derived cobalt-based nanoporous carbon (Co-NPC) for incorporation into poly(vinylidene fluoride) (PVDF) composite nanofibers	19.24	12
Rahman et al.[12]	ZIF-8 reinforcing nanofiller into poly(acrylamide)-*co*-hydroxyethyl acrylate (PAAm-*co*-HEA) hydrogel with LiCl electrolyte	3.47	4
Navaneeth et al.[13]	saline bottle sheets (polyethylene)	8.78	5
Karabiber et al.[23]	MoS_2 and WS_2 as separate additives into PAN composite nanofibers	25.3	2
Topçu et al.[22]	natural boron minerals (NBO) doped silicone	32.03	2
current work	long-lasting Scotch tape and box-lock Scotch tape (exploring the interaction between acrylic adhesive and polypropylene backing layers)	15.14	40
		8.57	150
		0.43	300

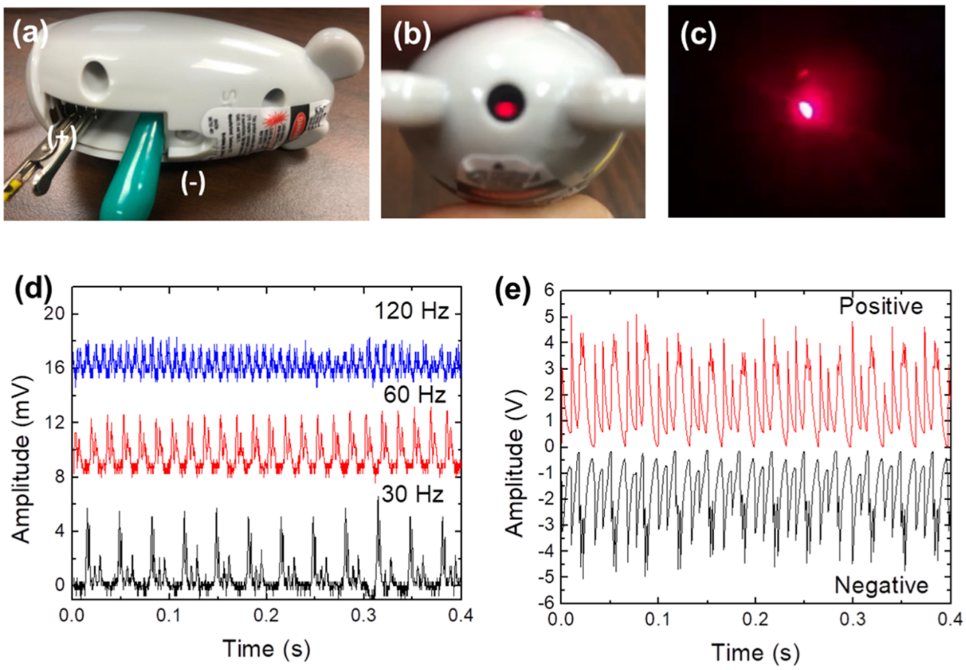

Figure 7. (a) Laser pointer with two electric wires. Laser light emission at a VBEH frequency of 30 Hz (b) with room light and (c) without room light. (d) Amplitude variation of the photodetector at 30, 60, and 120 Hz VBEH frequencies. (e) Amplitude change of two output terminals of the bridge rectifier at a 30 Hz VBEH frequency.

(Movie S2), (Movie S3), and (Movie S4), respectively. It is worth noting that our VBEH provides very powerful LED lighting even at a very high frequency of 150 Hz, thus broadening the field of applications for the proposed Scotch-based triboelectric generator. By replacing the LED with a laser diode (wavelength at 650 nm) with the same circuit configuration, we observed that the laser light turned on at different frequencies. In our previous study, we used double-sided tape triboelectric generators to determine laser illumination at 20 Hz.[14] In Figure 7(a), two wires were connected directly to the laser diode instead of to the coin battery. These wires distributed electricity from the two terminals of the bridge rectifier.[14] Figure 7(b),(c) shows the lasing of the diode at 30 Hz with and without room lighting. As shown in Figure 7(d), the current design allows for much higher frequencies; therefore, lasing at higher frequencies was detected by the photodetector. Laser-induced amplitude changes were observed at 30, 60, and 120 Hz. Video clips for laser illumination are shown in (Movie S5) and (Movie S6) for 30 and 60 Hz, respectively. The electrical amplitude change at 30 Hz resulting directly from the positive and negative terminals of the bridge diode is shown in Figure 7(e). As a result, laser illumination was confirmed even at 120 Hz, which provides good insight into triboelectric generators for optoelectronic applications.

In our previous study, we proposed a self-powered wearable biosensor using a single layer of Scotch tape, which was attached to the skin to conduct muscle activation measurements.[17] Potential skin irritation or skin conditions (e.g., sweat) could degrade the sensor's performance. We extended the current triboelectric generator design to the same biosensing application. Figure 8(a) shows a side view of the new sensor design schematic. Two layers of long-lasting tapes (bottom) and box-lock tapes (top) faced each other with non-tacky surfaces. The sensor assembly was connected to two wires for signal collection and placed on top of a fabric wrapped around a person's forearm, as shown in Figure 8(b). Then, a covering fabric was wrapped around the top of the biosensor, as shown in Figure 8(c). Forearm muscles during flexion and extension of the arm and flexion and extension of the fingers were recorded by using a digital oscilloscope. Figure 8(d),(e) shows the collected signals due to arm flexion and extension. Note that the current biosensor prevents direct skin contact to eliminate potential sensing degradation. Two separate channels can record signals from the top and bottom electrodes very clearly. Moreover, fine motor finger movements can be recorded from this biosensor, as shown in Figure 8(f). Figure 8(g) shows finger biosensors mounted on four different fingers that are bonded on the surface of a glove. It is allowed to record four different signals through a multichannel digital oscilloscope. Therefore, this new biosensor design using long-lasting and box-lock tapes shows enhanced biosensing capability.

Additional investigation was conducted to determine acoustic sensing capabilities. As shown in Figure 9(a), the same triboelectric generation configuration of PET/Al/box-lock tape/box-lock tape: long-lasting tape/long-lasting tape/Al/PET combination was placed on a vertical stand to form an acoustic sensor with an active area of 50 mm × 50 mm. All layers were stacked together, and there were no spacers among those layers. The signal wire was connected to the Al electrode on the long-lasting tape side, and the ground wire was connected to the Al electrode on the box-lock tape side. A digital oscilloscope was used to record collected voltage signals. A bluetooth speaker was placed in front of the acoustic sensor at various distances. License-free music from YouTube played on the speaker.[24] In Figure 9(b), the peak amplitude reached higher than 20 V when the speaker was in direct contact with the sensor. As shown in Figure 9(c), the amplitude decreases significantly as the distance between the sensor and the speaker. When the distance reaches 80 mm, the collected signal is almost negligible. We were able to replay recorded

https://doi.org/10.1021/acsomega.4c08590
ACS Omega 2025, 10, 2778−2789

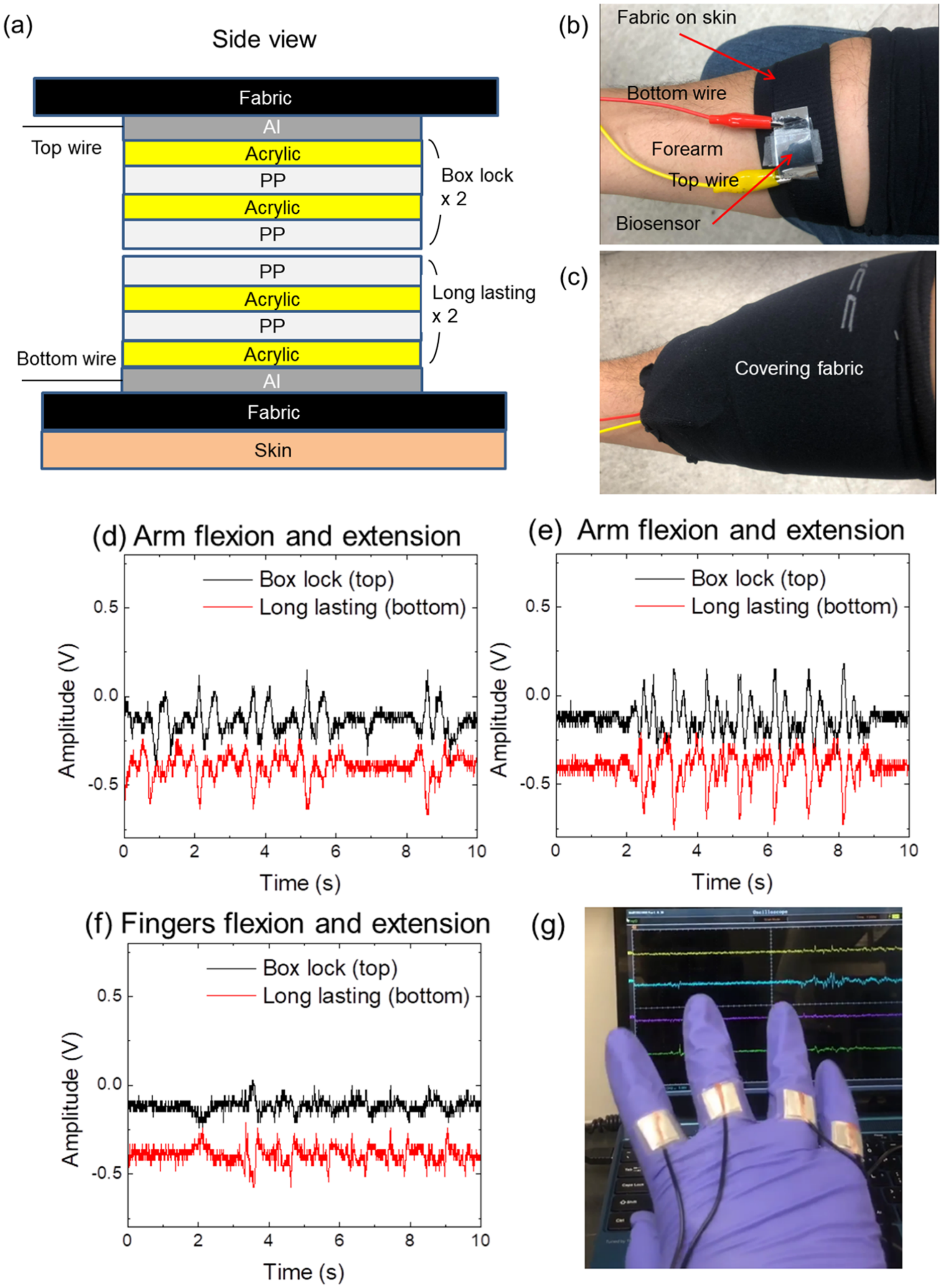

Figure 8. (a) Side view of the biosensor with two layers of long-lasting tape and box-lock tape. (b) Sensor is located on the top of the fabric wrapped around the person's forearm. (c) Top of the sensor is covered with another fabric. Amplitude plotted as a function of time for (d-e) arm flexion and extension, (f) finger flexion and extension, and (g) finger sensors built on the glove.

signals via a preamplifier. Preamplified signals at a distance of 40 mm were played on a laptop via the auxiliary connector, which demonstrates the near-field microphone capability with background noise cancellation. Additionally, when the sensor touches the speaker directly and music is played from the speaker, the LED lights that are connected to the sensor turn on as shown in (Movie S7).

CONCLUSIONS

In this Letter, we proposed a novel Scotch tape triboelectric generator and integrated it into a VBEH system. Such a

https://doi.org/10.1021/acsomega.4c08590
ACS Omega 2025, 10, 2778−2789

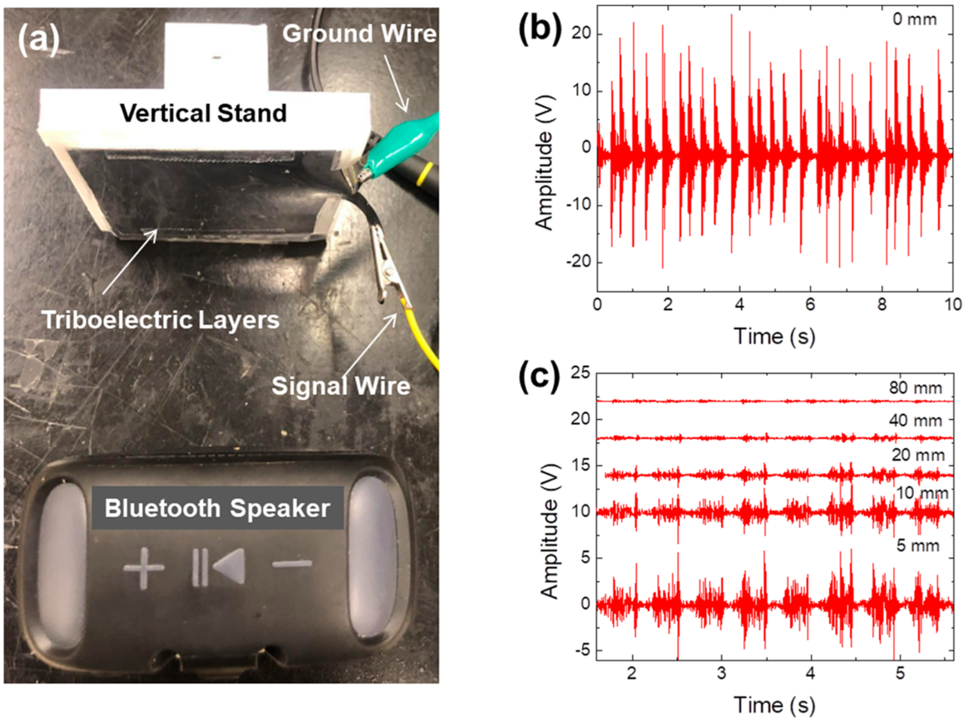

Figure 9. (a) Photo of the acoustic sensor setup using PET/Al/box-lock tape/box-lock tape: long-lasting tape/long-lasting tape/Al/PET on a 3D-printed vertical stand. Sound comes out of the Bluetooth speaker. (b) Voltage amplitude of the triboelectric layer without a gap between the triboelectric layer and the speaker. (c) Voltage amplitude of the triboelectric layer with distances of 5, 10, 20, 40, and 80 mm between the triboelectric layer and the speaker.

triboelectric generator design requires only a simple fabrication approach. The physics behind the triboelectrification is to explore atomic gaps between the polypropylene material and the acrylic adhesive layer in the tape. A multiple-layer design scheme allowed us to extract more power from the vibration. In addition, the tacky surface does not appear on the contact—separation interface, which allows a higher frequency operation. The operational frequency in our VBEH is up to 300 Hz, which is significantly higher than that of any TENG device in the literature. The triboelectric generator design with two layers of Scotch box-lock tape as one triboelectric layer assembly interfaces two Scotch long-lasting tape layers leads to the highest peak power extraction, which is 53 mW at 40 Hz.

Additionally, the physiological biosensor was manufactured with PET/Al/long-lasting tape/long-lasting tape − box-lock tape/box-lock tape/Al/PET configuration. The sensor is placed without direct contact with the skin. Moreover, an acoustic sensor with a current triboelectric design can be used as a short-distance microphone with potential noise cancellation.

In summary, we demonstrated the Scotch tape-based triboelectric generator concept in terms of energy harvesting in a VBEH system, muscle activation tracking in a wearable biosensor, and acoustic sensing in a microphone prototype. We expect that this simple design could lead to more engineering applications.

■ ASSOCIATED CONTENT

Supporting Information

The Supporting Information is available free of charge at https://pubs.acs.org/doi/10.1021/acsomega.4c08590.

Power versus time plots for PET/Al/long-lasting tape/long-lasting tape − box-lock tape/box-lock tape/Al/PET configuration VBEH with various resistance values from 1 to 40 MΩ (Figure S1) (PDF)

Video to show a triboelectric generator under a VBEH test from 30 to 10 Hz (Movie S1) (MP4)

Video to show a direct power of 148 LEDs using a VEBH triboelectric generator (PET/Al/long-lasting tape/long-lasting tape − box-lock tape/box-lock tape/Al/PET) driven by a shaker at 150 Hz (Movie S2) (MP4)

Video to show a direct power of 296 LEDs using a VEBH triboelectric generator (PET/Al/long-lasting tape/long-lasting tape − box-lock tape/box-lock tape/Al/PET) driven by a shaker at 20 Hz (Movie S3) (MP4)

Video to show a direct power of 366 LEDs using a VEBH triboelectric generator (PET/Al/long-lasting tape/long-lasting tape − box-lock tape/box-lock tape/Al/PET) driven by a shaker at 40 Hz (Movie S4) (MP4)

Video to show a direct power of a 650 nm diode laser using a VBEH triboelectric generator Video to show a direct power of a 650 nm diode laser using a triboelectric generator (PET/Al/long-lasting tape/long-lasting tape − box-lock tape/box-lock tape/Al/PET) driven by a shaker at 30 Hz (Movie S5) (MP4)

Video to show a direct power of a 650 nm diode laser using a VBEH triboelectric generator Video to show a direct power of a 650 nm diode laser using a triboelectric generator (PET/Al/long-lasting tape/long-lasting tape − box-lock tape/box-lock tape/Al/PET) driven by a shaker at 60 Hz (Movie S6) (MP4)

(Movie)S7: When the triboelectric acoustic sensor (PET/Al/long-lasting tape/long-lasting tape − box-

https://doi.org/10.1021/acsomega.4c08590
ACS Omega 2025, 10, 2778−2789

lock tape/box-lock tape/Al/PET) touches the speaker while music is playing, the LED lights turn on (Movie S7) (MP4)

AUTHOR INFORMATION

Corresponding Authors

Moon-Hyung Jang − *Department of Mechanical and Aerospace Engineering, The University of Alabama in Huntsville, Huntsville, Alabama 35899, United States; Department of Chemical and Materials Engineering, The University of Alabama in Huntsville, Huntsville, Alabama 35899, United States*; Email: moonhyung.jang@uah.edu

Gang Wang − *Department of Mechanical and Aerospace Engineering, The University of Alabama in Huntsville, Huntsville, Alabama 35899, United States*; orcid.org/0000-0001-9843-5966; Email: gang.wang@uah.edu

Authors

[‖]**Sean P. Rabbitte** − *Department of Mechanical and Aerospace Engineering, The University of Alabama in Huntsville, Huntsville, Alabama 35899, United States*

Abdelkader Frendi − *Department of Mechanical and Aerospace Engineering, The University of Alabama in Huntsville, Huntsville, Alabama 35899, United States*

Ryan T. Conners − *Department of Kinesiology, The University of Alabama in Huntsville, Huntsville, Alabama 35899, United States*

Yu Lei − *Department of Chemical and Materials Engineering, The University of Alabama in Huntsville, Huntsville, Alabama 35899, United States*; orcid.org/0000-0002-4161-5568

Complete contact information is available at: https://pubs.acs.org/10.1021/acsomega.4c08590

Author Contributions

M.-H.J. performed VBEH tests, FTIR measurements, LED tests, laser tests, biosensor tests, and acoustic sensor tests. M.-H.J., S.P.R., and G.W. proposed the VBEH design. M.-H.J. analyzed the data. M.-H.J., Y.L., A.F., R.T.C., and G.W. discussed the results. M.-H.J. and G.W. prepared the manuscript.

Notes

The authors declare no competing financial interest.
[‖]Graduated, now Systems Engineer at Lockheed Martin Space, Huntsville, 35805, AL

ACKNOWLEDGMENTS

This project is partially sponsored by the Charger Innovation Fund (CIF) at the University of Alabama in Huntsville.

REFERENCES

(1) Luo, J.; Wang, Z. L. Recent progress of triboelectric nanogenerators: From fundamental theory to practical applications. *EcoMat* **2020**, *2* (4), No. e12059.

(2) Dong, K.; Wu, Z.; Deng, J.; Wang, A. C.; Zou, H.; Chen, C.; Hu, D.; Gu, B.; Sun, B.; Wang, Z. L. A Stretchable Yarn Embedded Triboelectric Nanogenerator as Electronic Skin for Biomechanical Energy Harvesting and Multifunctional Pressure Sensing. *Adv. Mater.* **2018**, *30* (43), No. 1804944.

(3) Tang, Q.; Yeh, M.-H.; Liu, G.; Li, S.; Chen, J.; Bai, Y.; Feng, L.; Lai, M.; Ho, K.-C.; Guo, H.; Hu, C. Whirligig-inspired triboelectric nanogenerator with ultrahigh specific output as reliable portable instant power supply for personal health monitoring devices. *Nano Energy* **2018**, *47*, 74−80.

(4) Li, Z.; Feng, H.; Zheng, Q.; Li, H.; Zhao, C.; Ouyang, H.; Noreen, S.; Yu, M.; Su, F.; Liu, R.; et al. Photothermally tunable biodegradation of implantable triboelectric nanogenerators for tissue repairing. *Nano Energy* **2018**, *54*, 390−399.

(5) Liu, Z.; Li, H.; Shi, B.; Fan, Y.; Wang, Z. L.; Li, Z. Wearable and Implantable Triboelectric Nanogenerators. *Adv. Funct. Mater.* **2019**, *29* (20), No. 1808820.

(6) Huang, C.; Chen, G.; Nashalian, A.; Chen, J. Advances in self-powered chemical sensing via a triboelectric nanogenerator. *Nanoscale* **2021**, *13* (4), 2065−2081.

(7) Wang, Z. L.; Wu, W. Nanotechnology-Enabled Energy Harvesting for Self-Powered Micro-/Nanosystems. *Angew. Chem., Int. Ed.* **2012**, *51* (47), 11700−11721.

(8) Wang, Y.; Yang, Y.; Wang, Z. L. Triboelectric nanogenerators as flexible power sources. *npj Flexible Electron.* **2017**, *1* (1), No. 10.

(9) Liu, W.; Wang, Z.; Wang, G.; Liu, G.; Chen, J.; Pu, X.; Xi, Y.; Wang, X.; Guo, H.; Hu, C.; Wang, Z. L. Integrated charge excitation triboelectric nanogenerator. *Nat. Commun.* **2019**, *10* (1), No. 1426.

(10) Pandey, P.; Thapa, K.; Ojha, G. P.; Seo, M.-K.; Shin, K. H.; Kim, S.-W.; Sohn, J. I. Metal-organic frameworks-based triboelectric nanogenerator powered visible light communication system for wireless human-machine interactions. *Chem. Eng. J.* **2023**, *452*, No. 139209.

(11) Rahman, M. T.; Rana, S. M. S.; Zahed, M. A.; Lee, S.; Yoon, E.-S.; Park, J. Y. Metal-organic framework-derived nanoporous carbon incorporated nanofibers for high-performance triboelectric nanogenerators and self-powered sensors. *Nano Energy* **2022**, *94*, No. 106921.

(12) Rahman, M. T.; Rahman, M. S.; Kumar, H.; Kim, K.; Kim, S. Metal-Organic Framework Reinforced Highly Stretchable and Durable Conductive Hydrogel-Based Triboelectric Nanogenerator for Biomotion Sensing and Wearable Human-Machine Interfaces. *Adv. Funct. Mater.* **2023**, *33* (48), No. 2303471.

(13) Navaneeth, M.; Potu, S.; Babu, A.; Lakshakoti, B.; Rajaboina, R. K.; Kumar K, U.; Divi, H.; Kodali, P.; Balaji, K. Transforming Medical Plastic Waste into High-Performance Triboelectric Nanogenerators for Sustainable Energy, Health Monitoring, and Sensing Applications. *ACS Sustainable Chem. Eng.* **2023**, *11* (32), 12145−12154.

(14) Jang, M.-H.; Lee, J. D.; Lei, Y.; Chung, S.; Wang, G. Power Generation by a Double-Sided Tape. *ACS Omega* **2022**, *7* (46), 42359−42369.

(15) Jang, M.-H.; Rabbitte, S. P.; Lei, Y.; Chung, S.; Wang, G. Power Generation by a Limestone-Contained Putty. *ACS Omega* **2023**, *8* (10), 9326−9333.

(16) Zięba-Palus, J. The usefulness of infrared spectroscopy in examinations of adhesive tapes for forensic purposes. *Forensic Sci. Criminol.* **2017**, *2*, 1−9.

(17) Jang, M.-H.; Lei, Y.; Conners, R. T.; Wang, G. Self-powered triboelectric wearable biosensor using Scotch tape. *J. Mater. Chem. B* **2023**, *11* (44), 10640−10650.

(18) Zahedi, H.; Foroutan, M. Separation of water−oil mixture on poly methyl methacrylate surface using TiO2 nanoparticles via molecular dynamics simulation. *Adsorption* **2019**, *25* (5), 1019−1031.

(19) Camara, C. G.; Escobar, J. V.; Hird, J. R.; Putterman, S. J. Correlation between nanosecond X-ray flashes and stick−slip friction in peeling tape. *Nature* **2008**, *455* (7216), 1089−1092.

(20) Wang, H.; Xu, L.; Bai, Y.; Wang, Z. L. Pumping up the charge density of a triboelectric nanogenerator by charge-shuttling. *Nat. Commun.* **2020**, *11* (1), No. 4203.

(21) Chung, J.; Heo, D.; Shin, G.; Choi, D.; Choi, K.; Kim, D.; Lee, S. Ion-Enhanced Field Emission Triboelectric Nanogenerator. *Adv. Energy Mater.* **2019**, *9* (37), No. 1901731.

(22) Topçu, M. A.; Karabiber, A.; Koç, F.; Sarılmaz, A.; Özel, F. Boron Minerals with Different Crystal Structures as Performance Manipulators in Triboelectric Nanogenerators. *Energy Technol.* **2024**, *12* (4), No. 2301282.

https://doi.org/10.1021/acsomega.4c08590
ACS Omega 2025, 10, 2778−2789

(23) Karabiber, A.; Dirik, Ö.; Okbaz, A.; Yar, A.; Özen, A.; Özel, F. Transition Metal Dichalcogenides as Effective Dopants in Nanofiber-Based Triboelectric Nanogenerators. *Int. J. Energy Res.* **2024**, *2024* (1), No. 8838934.
(24) https://www.youtube.com/watch?v=M7feDIHL3qc. (accessed May 24, 2024).

https://doi.org/10.1021/acsomega.4c08590
ACS Omega 2025, 10, 2778−2789